Accepted Manuscript

Early-stage photodegradation of aromatic poly(urethane-urea) elastomers

Tianlong Zhang, Fengwei Xie, Julius Motuzas, Peter Bryant, Valsala Kurusingal, John M. Colwell, Bronwyn Laycock

PII: S0141-3910(18)30300-8

DOI: 10.1016/j.polymdegradstab.2018.09.020

Reference: PDST 8645

To appear in: *Polymer Degradation and Stability*

Received Date: 15 January 2018

Revised Date: 11 September 2018

Accepted Date: 25 September 2018

Please cite this article as: Zhang T, Xie F, Motuzas J, Bryant P, Kurusingal V, Colwell JM, Laycock B, Early-stage photodegradation of aromatic poly(urethane-urea) elastomers, *Polymer Degradation and Stability* (2018), doi: https://doi.org/10.1016/j.polymdegradstab.2018.09.020.

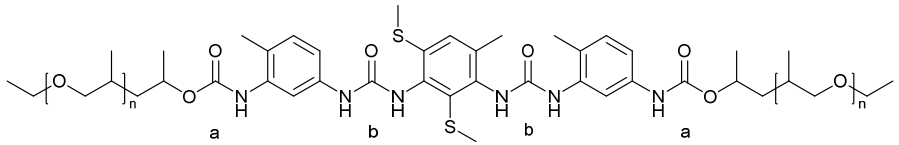

PUU

PUU

PUU-C3

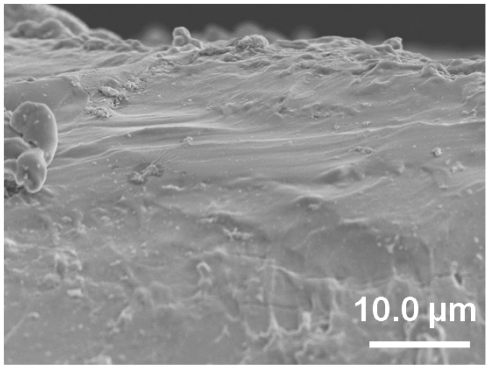

60 h UV ageing

Evaluation of high-structure carbon black's UV protection for PUU sample (PUU-C3)

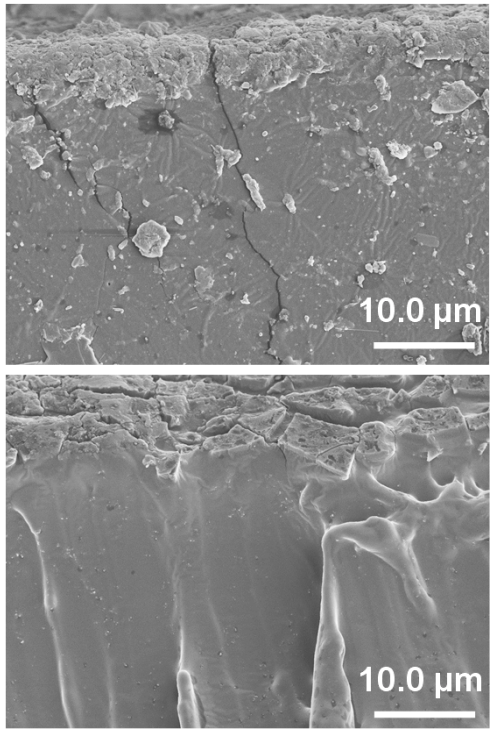

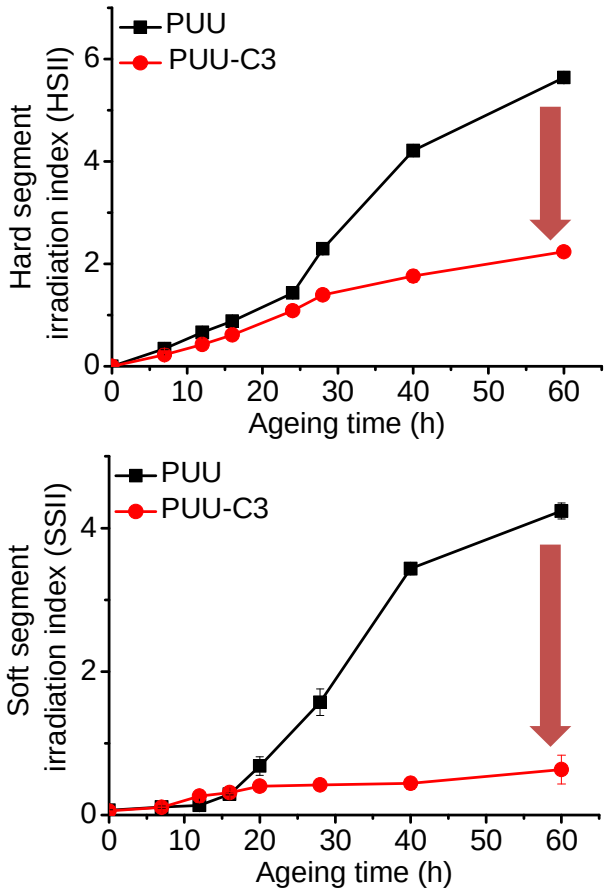

Significantly decrease in irradiation indices

Early-stage photodegradation of aromatic poly(urethane-urea) elastomers

Tianlong Zhang [a,b], Fengwei Xie [a,b,c,d,*], Julius Motuzas [a], Peter Bryant [e], Valsala Kurusingal [e], John M. Colwell [b,f], Bronwyn Laycock [a,b,†]

[a] *School of Chemical Engineering, The University of Queensland, Brisbane, Qld 4072, Australia*

[b] *Defence Materials Technology Centre (DMTC), Level 2, 24 Wakefield St., Hawthorn, Vic 3122, Australia*

[c] *Institute of Advanced Study, University of Warwick, Coventry CV4 7HS, United Kingdom*

[d] *International Institute for Nanocomposites Manufacturing (IINM), WMG, University of Warwick, Coventry CV4 7AL, United Kingdom*

[e] *Thales Australia, Rydalmere, NSW 2116, Australia*

[f] *School of Chemistry, Physics and Mechanical Engineering, Science and Engineering Faculty, Queensland University of Technology (QUT), GPO Box 2434, Brisbane, QLD, Australia*

[*] Corresponding author. Email: f.xie@uq.edu.au; fwhsieh@gmail.com (F. Xie)

[†] Corresponding author. Email: b.laycock@uq.edu.au (B. Laycock)

Abstract:

The photooxidative stability of an aromatic segmented poly(urethane-urea) (PUU) elastomer, stabilised with a range of carbon black fillers, was assessed after very low UVA doses as a means to identify components that are highly susceptible to UV degradation, and suggest better design of such materials. Fourier-transform infrared (FTIR) analysis indicated rapid degradation of the urea bonds in the hard segments, followed by chain scission and photo-Fries reaction of the urethane linkages. In the soft segments, the oxidation of the original ether groups resulted in the formation of large amounts of ester groups, while some crosslinking of the ether groups was also evident. Carbon black provided moderate protection against degradation, with the smallest-sized particles being the most effective. Protection was evidenced by reduced surface cracking as well as an increased resistance to chemical changes in both the soft segments and hard segments. Even so, significant degradation was still evident at low UV doses suggesting that further stabilisation is required to increase the UV durability of these elastomers and improve their long-term performance.

Keywords: UV ageing; aromatic poly(urethane-urea); carbon black

1 Introduction

Poly(urethane-urea) (PUU) is a type of polyurethane (PU) block copolymer formed using diamines as the chain extenders and crosslinking agents. This group of polymers is considered to have a more complicated structure and increased hydrogen-bonding properties relative to other PUs since there are two different type of N-H bonds present in the urethane and urea linkages [10]. For the production of PUUs, both aromatic and aliphatic diamines can be used, such as 4,4′-methylenebis(2-chloroaniline) (MOCA), [11] diethyltoluenediamine (DETDA) [12], and 2,4-diamino-3,5-dimethylsuphylchlorobenzene (DDSCB) [10]. The addition of these diamine chain extenders is supposed to improve thermal stability and mechanical properties since, compared with PUs, PUU elastomers have higher cohesive linkages through the urea groups in the hard segments [13-16]. PUU elastomers are widely used for marine, aircraft and biomedical applications due to their low glass transition temperatures (T_g), high flexibility and outstanding biocompatibility [17, 18]. However, PU-based elastomers are generally considered to be extremely susceptible to ultraviolet (UV) irradiation, resulting in irreversible changes in their structure and chemistry, which largely affect their physical and mechanical properties [9]. Thus, there has been a rising interest in finding a cost-effective method to improve the UV stability of PU elastomers to extend their lifetime and maintain their performance when exposed to aggressive environments.

The mechanism of PUU photodegradation is complicated, as several photolytic reactions can occur at the same time, such as the oxidation-induced discolouration of aromatic urethane/urea groups, chain scission and oxidation of the polyol segment, and breakage of N–H bonds in the system. PUUs have been found to exhibit better photostability than their polyurea counterparts [19]. However, due to limited work in this area, a complete description of the PUU photodegradation process and how the UV irradiation affects the properties of PUU remain unclear.

For practical applications, there is an urgent need to find cost-effective techniques to improve the UV stability of PUUs. While the use of different additives/stabilisers in PUs and PUUs to enhance their photostability has been widely reported, carbon black has been found to be the most viable choice since it can absorb UV over a wide range of wavelengths and is not consumed during service [20]. Carbon black is one of the most commonly used and effective UV stabilisers in polymer applications, being the major additive providing UV protection for plastics such as outdoor wire and cable jacketing, pipes, and geosynthetic membranes [21, 22]. For polyethylene (PE), for example, a loading of 2–3% by weight of carbon black should provide effective UV protection [22-24]. By absorbing and scattering UV, well-dispersed carbon black can largely reduce the dosage of UV irradiation to polymers, thus greatly reducing the photoinduced structural and property changes [21].

It is worth noting that the primary particle size, structure, surface chemistry, and dispersion state of carbon black could significantly influence the effectiveness of the UV protection provided [25]. Generally, smaller particles and aggregate sizes bring better stabilisation because of the increased surface area for intercepting UV [26]. However, when the sizes of the carbon black particles and primary aggregates become too small (less than 20–25 nm), light scattering, especially forward scattering, becomes more important, which may have a negative effect on the UV stability of the polymer [21]. It is also known that carbon black with small particle sizes usually have a higher tendency to agglomerate into clusters, which are difficult to disperse in polymers [26]. Therefore, the structural features of carbon black play a significant role in the UV stabilisation of polymers.

The present work focuses on the photodegradation pathways of a segmented PUU elastomer based on an aromatic isocyanate and a polyether during the early stage of UV ageing (60 h). The effects of three types of carbon black with different structural characteristics on the UV stability of this PUU were also studied. The photodegradation processes were analysed using Fourier-transform infrared (FTIR) studies of the PUU surface chemistry over the monitoring period, along with other techniques such as scanning electron microscopy (SEM), X-ray photoelectron spectroscopy (XPS),

and differential scanning calorimetry (DSC), which were used to analyse the surface features and property changes before and after UV ageing. Thus, this work provides further mechanistic understanding of the photodegradation of PUU elastomers, which is expected to guide future work on the development of high-performance PUU composite materials with enhanced weathering stability.

2 Materials and methods

2.1 Materials

A two-pack commercial PUU product, "NUWC XP-1 Polyurethane Encapsulant", was purchased from Alfa International Corporation (Woonsocket, RI, USA). This PUU has been reported in the literature for use in marine applications [27]. Part A of this formulation is a prepolymer resulting from the reaction between polyether polyols and toluene diisocyanate (TDI). The polyether is polypropylene glycol (PPG), with an average molecular weight (M_w) of 1500 g/mol, achieved by mixing polyether polyols with molecular weights of 1000 and 2000 g/mol together. The TDI is a mixture of 80% toluene 2,4-diisocyanate and 20% toluene 2,6-diisocyanate. Part B is dimethylthiotoluenediamine (DMTDA), which is the curing agent. The recommended mixing ratio of the prepolymer (Part A) to the curing agent (Part B) is 100 to 11.5 parts by weight.

Three types of carbon black were used, including BP460 (Cabot Malaysia), N660 (Cabot Malaysia), and H30253 Super P® Conductive 99+% (metals basis) (Alfa Aesar, UK). These types of carbon black were coded as C1, C2, and C3, respectively.

2.2 Poly(urethane-urea) preparation

PUU films were prepared using a casting method. Firstly, carbon black was added into Part A and dispersed using a tip-probe sonicator (VC-505, 500 watts, 20 kHz, Sonics & Materials, Inc., Newtown, CT, USA). For the sonication, 12 pulsing cycles of 10 min with an amplitude of 20% were used. Between each cycle, there was a 30 min break to prevent the mixture from overheating. After sonication, the mixture was degassed in a vacuum chamber to −100 kPa for at least 200 min at room temperature until no air remained in the mixture (as identified by the absence of air bubbles escaping). Part B was then added into Part A and the mixture was stirred at 2000 rpm for 2 min using a stand drill mixer equipped with a propeller before undergoing a second degassing cycle in the vacuum chamber for 30 min. The weight ratio of Part A : Part B : carbon black was 100 : 11.5 : 0.56 (carbon black shared 0.5% of the total weight). The degassed PUU mixture was then carefully poured into flat moulds for curing. The moulds had been sprayed with silicone as a mould release agent and heated for 1 h at 80°C before use. After the materials had set (≥20 h), the solid PUU samples were removed from the moulds and cured in a 60°C oven for about 24 h as an accelerated curing step, and further stabilised for over 7 days at room temperature before any characterisation work. A blank PUU sample (without carbon black) was also made following the same procedure for comparison purposes.

2.3 Accelerated UV ageing

Samples were cut from 2.5–3.5 mm thick flat sheets and loaded into custom-built extensometers according to ASTM D1149–16 using Method B, Procedure B1 – Straight Specimens (Static Elongation). The accelerated ageing method was adapted from UV Resistance MIL–STD–810G, Method 505.5, Procedure II (A2). Briefly, samples were loaded into a QUV accelerated weathering tester (Q-Lab, Ohio, USA) that was equipped with UVA-340 lamps. The samples were held at 50°C

and were exposed to a UV intensity of 0.73 W/m^2 at 340 nm on the sample surfaces (The UVA dose was calibrated by a CR10 calibration radiometer every week). After 60 h of UVA ageing, samples received a total UVA dose of 157.68 kJ/m^2 at 340 nm.

2.4 Characterisation

2.4.1 Scanning electron microscopy (SEM)

The morphological features of the carbon black powders and PUU samples were examined using a JEOL JSM-7001F scanning electron microscope (SEM) with an accelerating voltage of 5 kV, a working distance of 10 mm and a spot size of 1. All samples were coated with platinum in an argon atmosphere to prevent charging during image acquisition.

2.4.2 N_2 adsorption

Carbon black porosity analysis was performed by nitrogen sorption using a Tristar II 3020 (Micromeritics). The samples were degassed under vacuum for 24 h at 200°C before measurement. The specific surface area and pore volume were calculated using the Brunauer–Emmett–Teller (BET) equation. The pore size distribution curves were determined using non-local density functional theory (NLDFT) from the desorption branch of the isotherms.

2.4.3 X-ray photoelectron spectroscopy (XPS)

Surface analysis was performed on a Kratos Axis ULTRA X-ray photoelectron spectrometer (XPS) using monochromatic Al Kα ($h\nu$ = 1486.6 eV) radiation. Curve fitting was undertaken using a Gaussian–Lorentzian peak shape and Shirley background function. The binding energy was

calibrated against the carbon signal at 284.6 eV. CasaXPS software was used to process the acquired data.

2.4.4 Attenuated total reflectance-Fourier-transform infrared (ATR-FTIR) spectroscopy

ATR-FTIR spectra of PUU samples were collected on a Nicolet 5700 Spectrometer (Thermo Electron Corporation) at a spectral resolution of 4 cm^{-1}, over the range 4000–400 cm^{-1} for a total of 32 scans. To check the consistency of the results, spectra were acquired at three separate spots on the surface of each sample. For the UV-aged samples, measurements were performed on the side that was towards the light during ageing. A self-cured Part A sample was also tested using the same method to help to identify the characteristic peaks in the FTIR spectra. Baseline correction was undertaken using OMNIC software (version 7.4.174). After baseline adjustment, the spectra were band-fitted using PeakFit software (version 4.12) and the fitted peak positions and areas calculated.

2.4.5 Differential scanning calorimetry (DSC)

A TA Q2000 DSC (TA Instruments, Inc., New Castle, DE 19720, USA) was used to investigate the thermal transitions of different PUU samples. 1.5–3 mg of each sample was weighed into 40 μL Tzero aluminium pans (TA Instruments). An empty pan was used as a reference. The pans underwent a three-stage run (from 30°C to 190°C; from 190°C to −90°C; and then from −90°C to 300°C) at 20°C/min. The instrument was calibrated using indium as a standard. At least three runs were undertaken for each sample to ensure the consistency of the results. Universal Analysis 2000 (TA Instruments–Waters LLC) software was used to analyse the thermal transitions from DSC traces.

3 Results and discussion

3.1 Carbon black characteristics

As discussed above, a smaller carbon black particle size generally delivers better protection for polymers against UV irradiation. In this study, three different types of carbon black, namely, BP460 (C1), N660 (C2) and Super P® Conductive (C3), were used. As seen from Fig. 1, C1 is formed from large chunks (1 μm) composed of smaller particulates 40–80 nm in size embedded in a glue-like material, while C2 and C3 show individual particles, of which the sizes were about 80–120 nm and 30–50 nm, respectively. For UV stabilisation applications, C2 and C3 are usually considered to be "high structure" carbon blacks, while C1 is a "low structure" carbon black with large agglomerates. The porosity of the three types of carbon black as determined by N_2 gas adsorption is shown in **Fig. S1** in **Supplementary Data** and the calculated surface areas are shown in Table 1 (note that these measurements usually have 10% experimental deviation). The data demonstrate that all of the carbon black types shared a similar pore size of 6–7 nm. C1 and C3 also have similar surface areas as determined by BET analysis. Meanwhile, the C2 sample presented a lower surface area. The observation correlates with the particulate size, where the smaller size of particles for C1 and C3 provide higher porosity compared to C2, which is composed of larger particles. In addition, as the sample C1 has the highest porosity, it seems that the glue-like material present in this sample is also highly porous. Further, the pore volume in the sample follows the rule that the larger pores provide greater pore volume; however, the surface area is lower. This tendency was observed between samples C1 and C3.

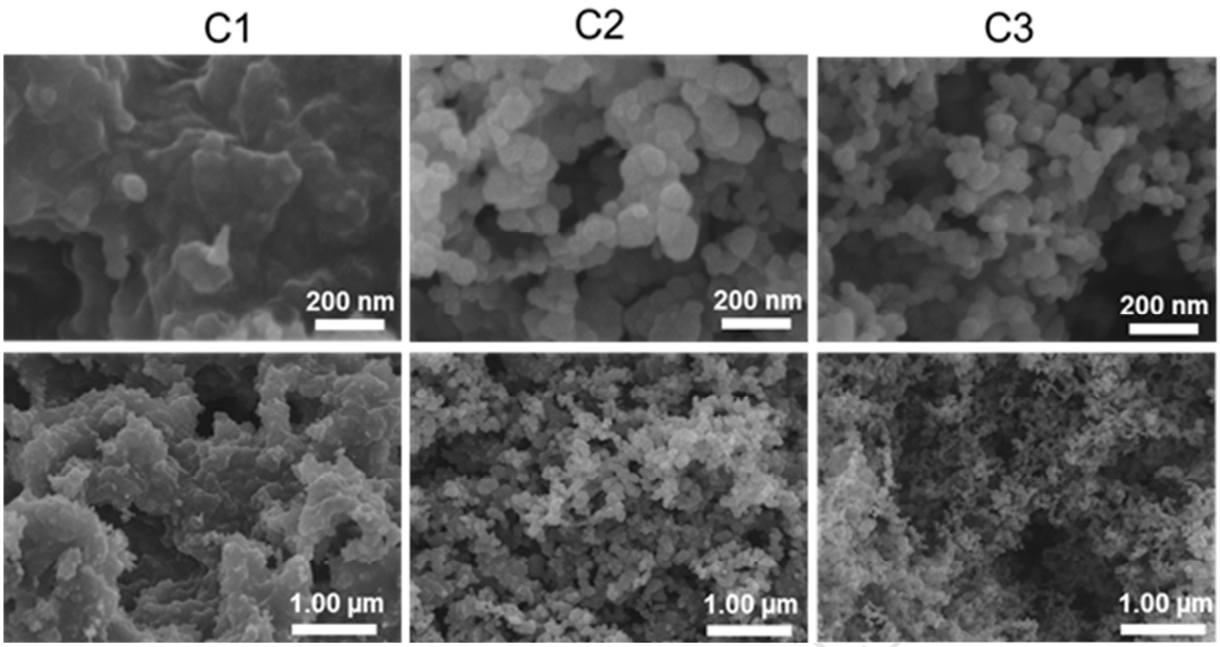

Fig. 1. SEM images of different carbon blacks.

Table 1. Surface area and porosity of different carbon blacks.

Carbon black	BET surface area (m^2/g)	Pore volume (cm^3/g)	Pore size (nm)
C1 – BP460	65.8	0.100	6.08
C2 – N660	33.6	0.052	6.16
C3 – Super P	62.5	0.113	7.26

3.2 Morphology of PUU samples

Fig. 2 shows the SEM images of cross-sections and normal surfaces of the blank PUU (carbon black-free), PUU-C1, PUU-C2 and PUU-C3 before and after UV ageing for 60 h. There was a slight difference in morphology between the unaged blank PUU and the PUU samples that contained carbon black. The cross-sectional images of PUU-C1 and PUU-C2 show a higher degree of roughness, while all the samples showed a smooth normal surface. For all the UV-irradiated samples, roughening and surface cracking were observed, with different levels of cracking being evident for

the different samples. The blank PUU showed the greatest extent of cracking, with a crack depth up to 30 μm. Carbon black-containing samples showed lower crack depths, but significant surface cracking. PUU-C3 was found to be least affected, with cracking isolated to its surface. A possible reason for its higher stability was better dispersion of the smaller carbon black particles (C3) in the polymer matrix, compared with that of C1, which had large agglomerates. Although PUU-C2 seems to have a smooth surface after UV irradiation, the cross section was rough, which suggests degradation extended into the bulk of the sample. From the data collected here, carbon black particle size and structure appear to be the main factors that influence the UV stability of this PUU elastomer.

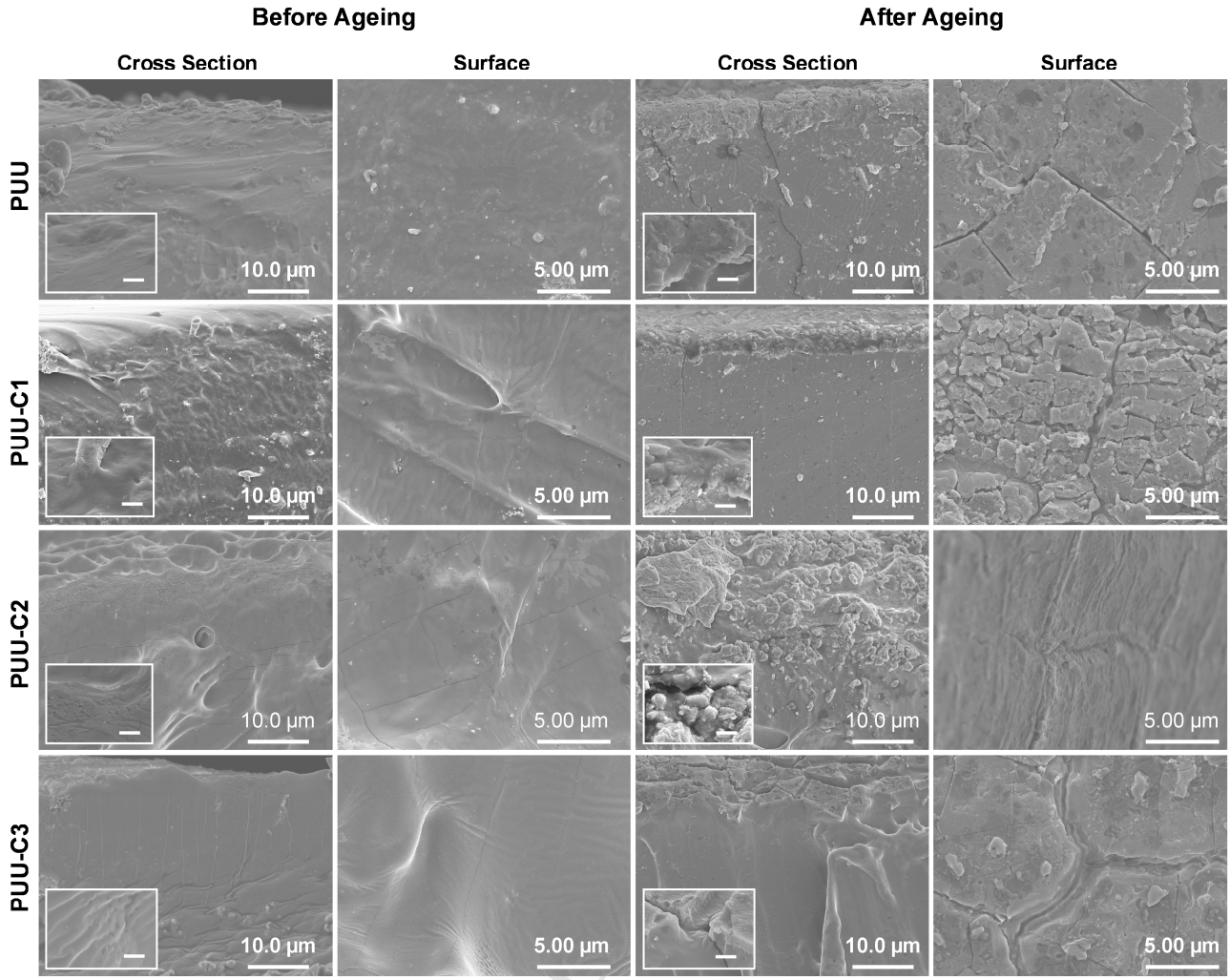

Fig. 2. SEM images of different PUU samples before and after 60 h of UV ageing. The scale bar in the insets is 1.00 µm.

3.3 XPS

X-ray photoelectron spectroscopy (XPS) was used to analyse the changes in the surface chemistry of PUU samples under UV irradiation in an examined area of 700 µm × 300 µm. Fig. 3 shows the changes in the O_{1s}/C_{1s} and N_{1s}/C_{1s} ratios for different samples before and after ageing (errors are expected to be around 2–5%). The ratios were calculated from the related peaks in the wide-scan XPS spectra (see **Fig. S2** in **Supplementary Data**). It is shown that the O_{1s}/C_{1s} and N_{1s}/C_{1s} ratios of all the samples were similar before UV ageing, suggesting that there was

consistency in the preparation of the materials. After UV irradiation, the O_{1s}/C_{1s} ratio of the blank PUU increased from 0.32 to 0.41, indicating that oxidation had occurred on the surface of the polymer [28, 29], which might be due to photooxidation of the aliphatic ether groups [30] Meanwhile, the N_{1s}/C_{1s} ratio increased from 0.05 to 0.11. After adding carbon black into the system, all the samples showed less UV-induced surface modification. Compared with the other samples, PUU-C3 (containing carbon black of the smallest particle size) seemed to have the least increase in both the O_{1s}/C_{1s} and N_{1s}/C_{1s} ratios, which rose from 0.32 to 0.33 and from 0.04 to 0.07, respectively. In contrast, for the PUU-C1 surface, the O_{1s}/C_{1s} ratio increased from 0.31 to 0.37 and the N_{1s}/C_{1s} ratio from 0.04 to 0.08. For the surface of PUU-C2, the O_{1s}/C_{1s} ratio changed from 0.30 to 0.39 and the N_{1s}/C_{1s} ratio from 0.04 to 0.09. The increases in both the O/C and N/C ratios on the surfaces of samples was possibly due to oxidation and loss of carbon during UV ageing (potentially through the formation of gaseous byproducts such as CO_2) [31-33]. These data show that PUU-C3 had the lowest degree of surface photooxidation after UV exposure, which, again, shows that C3 gave the most efficient protection against UV damage. In contrast, PUU-C2 showed a much higher degree of oxidation compared to PUU-C1 and PUU-C3, which indicates that a low surface area carbon black will largely reduce the UV stabilisation effect of this additive.

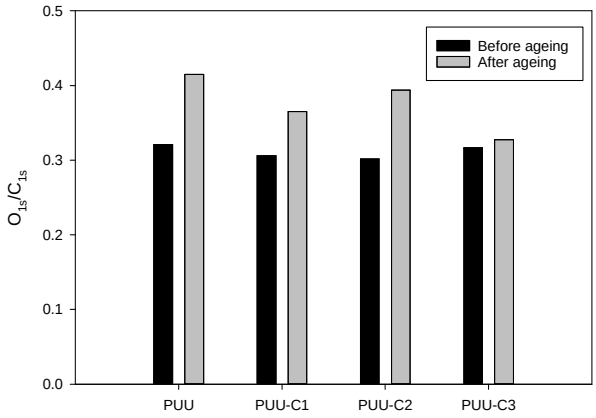

(a)

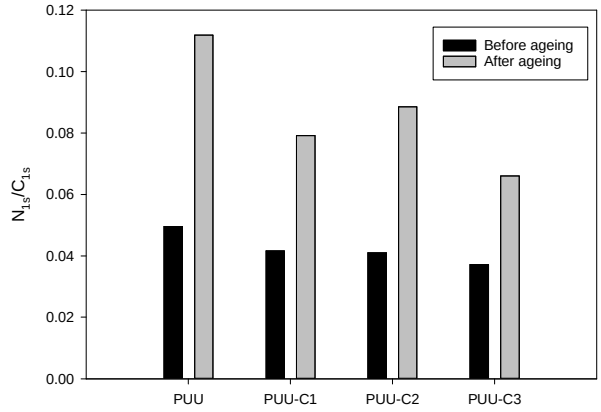

Fig. 3. O/C (a) and N/C (b) ratios for different PUU samples before and after UV ageing.

To further understand the surface changes during the photodegradation, high-resolution XPS spectra of the C_{1s} region were collected. All the spectra were calibrated using the reference C-C/C-H peak at 284.8 eV. Due to the complexity of the data collected, high-resolution C_{1s} spectra were band-fitted into a series of peaks corresponding to different functional groups. For the band fitting, the full width at half maximum (FWHM) was set between 1.1–1.3 eV. Fig. 4 shows the high-resolution C_{1s} spectra and one possible envelope curve fitting of the blank PUU, PUU-C1, PUU-C2 and PUU-C3 before and after UV ageing. The C_{1S} spectra of the unaged blank PUU revealed the presence of four

peaks, corresponding to C-C/C-H groups (284.8 eV), C-O groups (286.3 eV), C-N groups (287.9 eV), and C=O groups (287.6 eV) [29, 34-36]. After UV ageing, two new peaks were found at 285.5 eV and 288.6 eV. These peaks are likely to be linked to perester or anhydride groups, respectively. After adding carbon black, the generated perester/anhydride peaks were considerably lower in intensity, suggesting that the carbon black provided some protection against UV degradation for PUU.

(a)

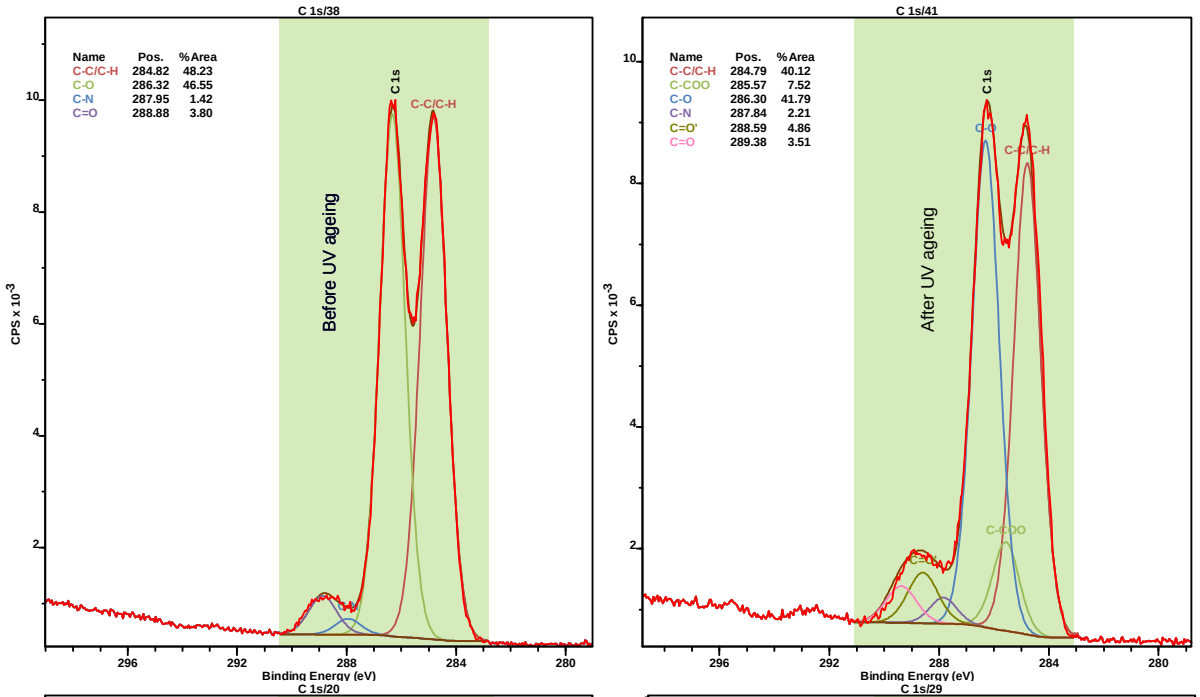
C 1s/38
Name Pos. %Area
C-C/C-H 284.82 48.23
C-O 286.32 46.55
C-N 287.95 1.42
C=O 288.88 3.80
Before UV ageing
C 1s
C-C/C-H
CPS x 10-3
Binding Energy (eV)
C 1s/41
Name Pos. %Area
C-C/C-H 284.79 40.12
C-COO 285.57 7.52
C-O 286.30 41.79
C-N 287.84 2.21
C=O' 288.59 4.86
C=O 289.38 3.51
After UV ageing
C-O
C-COO
C=O'

(b)

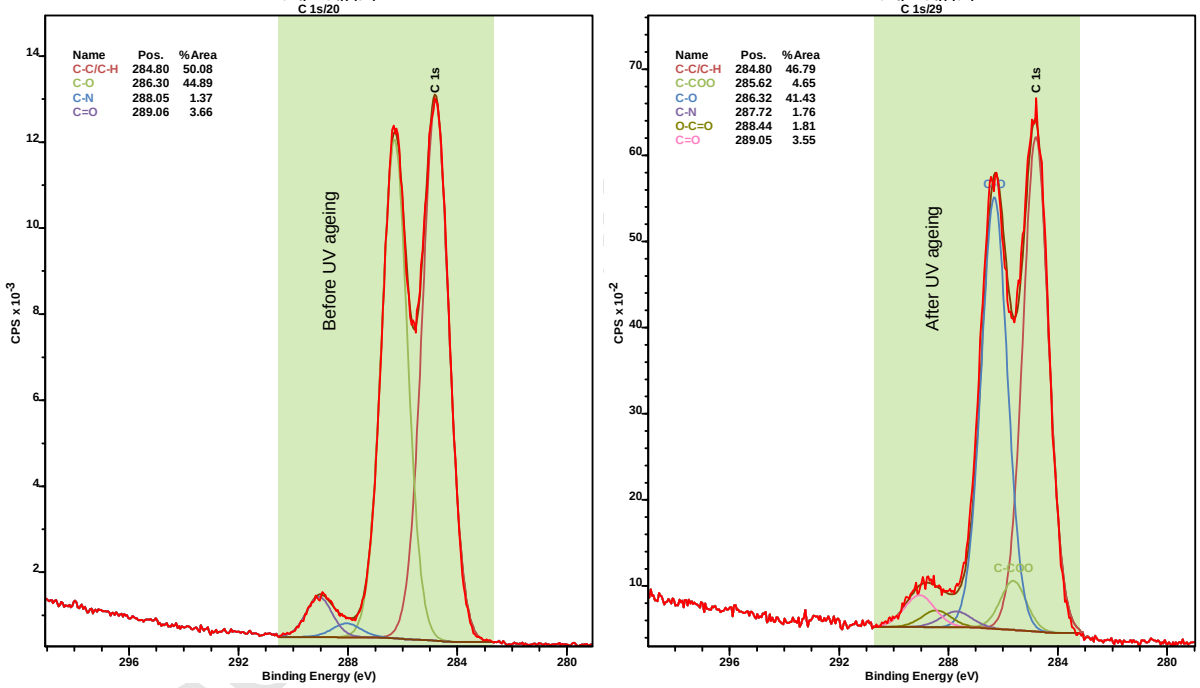
C 1s/20
Name Pos. %Area
C-C/C-H 284.80 50.08
C-O 286.30 44.89
C-N 288.05 1.37
C=O 289.06 3.66
Before UV ageing
C 1s
CPS x 10-3
Binding Energy (eV)
C 1s/29
Name Pos. %Area
C-C/C-H 284.80 46.79
C-COO 285.62 4.65
C-O 286.32 41.43
C-N 287.72 1.76
O-C=O 288.44 1.81
C=O 289.05 3.55
After UV ageing
C-O
C-COO
CPS x 10-2

258
259

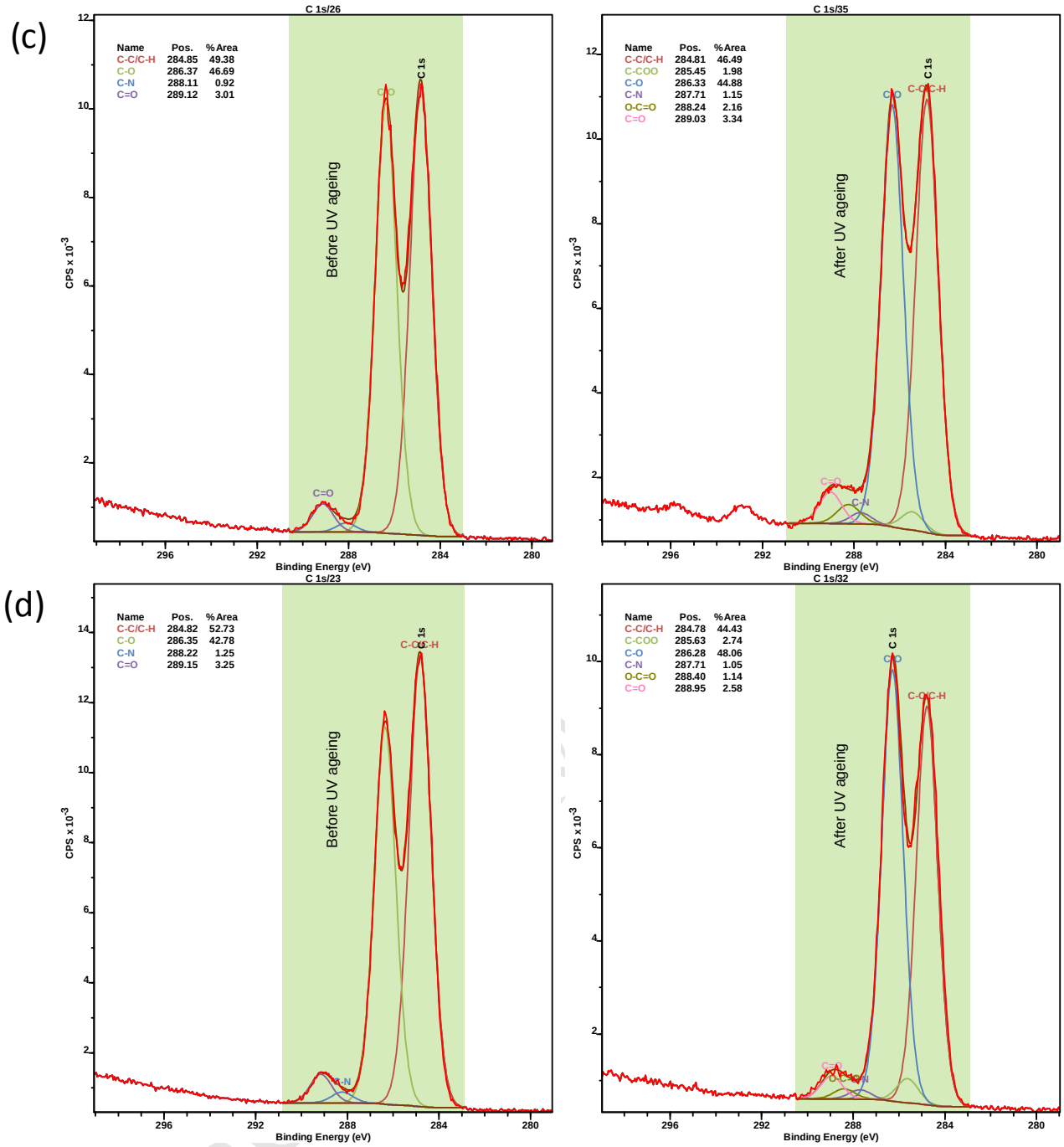

Fig. 4. C_{1s} spectra of PUU (a), PUU-C1 (b), PUU-C2 (c), and PUU-C3 (d) before and after UV ageing

3.4 FTIR

FTIR spectroscopy was used to further monitor the chemical changes on the surfaces of PUU samples after UV irradiation.

3.4.1 PUU band assignments

An FTIR-ATR spectrum from the blank PUU is shown in Fig. 5. Critical FTIR band assignments are listed in Table 2, which contains bands characteristic of both urethane and urea functional groups. This includes bands at: 3302 cm^{-1} (N-H stretching vibration, Amide A), 1727 cm^{-1} (C=O stretching vibration, Amide I), 1535 cm^{-1} (N-H deformation and C-N and C-C stretching vibration, Amide II), 1224 cm^{-1} (C-N stretching vibration, Amide III), 1634 cm^{-1} (stretching vibration of the C=O bond in the carbonyl group (-NH-CO-NH-) in diphenylurea [6, 37-40]), a shoulder at 1691 cm^{-1} (hydrogen-bonded carbonyls of the urethane group), a shoulder at 3250 cm^{-1} (stretching vibration of the N-H bond in the urea group or the hydrogen-bonded N-H bond in the urethane group), and a shoulder at 1261 cm^{-1} (C-N stretching vibration in the urea bond).

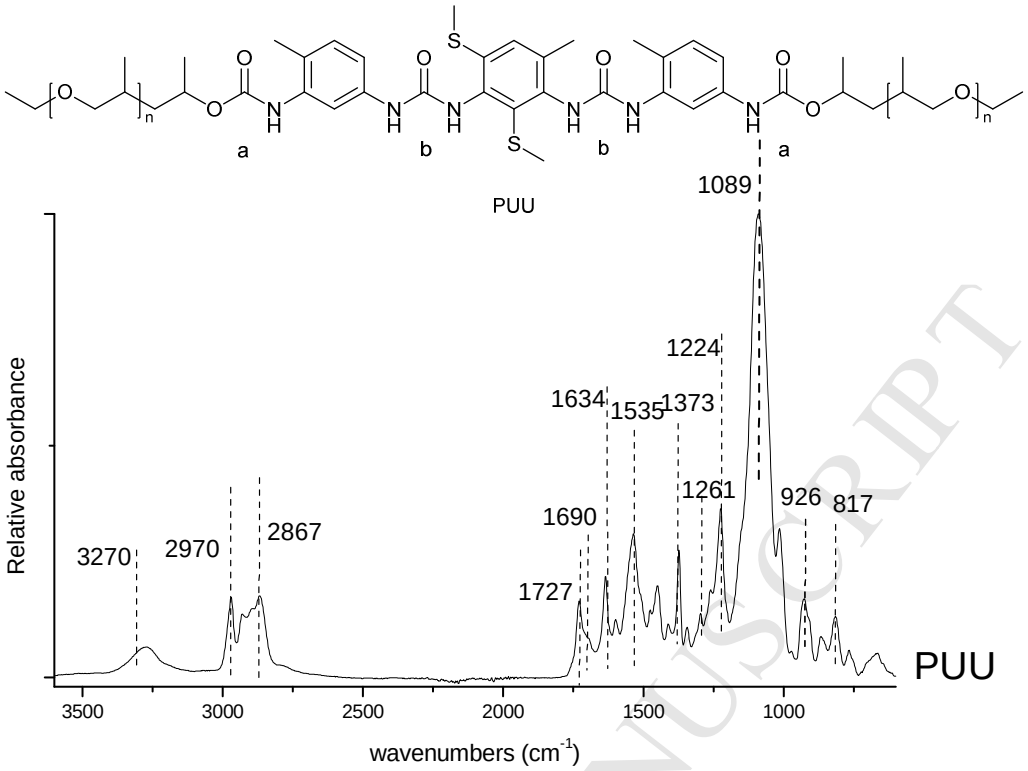

278

279 Fig. 5. FTIR spectrum from the blank PUU sample (unaged), shown below its chemical

280 structure.

281

282 Table 2. FTIR band assignments for PUU materials.

Peak centre (cm^{-1})	Relative intensity[a]	Assignment[b]
3302	vw, sh	υ (N-H) in urethane group (Amide A)
3270	vw, sh	υ (N-H) in urethane & urea group (free and hydrogen-bonded) combined
2970	m	υ^{as} ($-CH_3$)
2929	w	υ^{s} ($-CH_3$)
2902	w	υ^{as} ($-CH_2$)
2867	m	υ^{s} ($-CH_2$)
1728	s	υ (C=O) in urethane (Amide I)
1700	w, sh	υ (C=O) H-bonded
1634	s	υ (C=O) in diphenylurea group
1597	m	υ (C=C) in aromatic ring

1535	s	δ (N-H) + υ (C-N) + υ (C-C) Amide II in urethane & urea group combined
1449	m	δ ($-CH_2$)
1372	s	υ (C-N)
1261	w, sh	υ (C-N) in urea
1224	s	υ (C-N) in urethane (Amide III)
1089	vs	υ^{as} (C-O-C)
1013	s	υ^{s} (C-N) in amine [41]
927	s	υ^{s} (C-O-C) [41]
867	m	υ (C-O-C)/ρ ($-CH_2$) from ether [42]
815	w	δ_{oop} (C-H) in aromatic ring

[a] vw = very weak; w = weak; m = medium; s = strong; vs = very strong; sh = shoulder.

[b] υ, Stretching vibration; δ, in plane deformation vibration; δ_{oop}, out of plane deformation vibration

3.4.2 Effect of UV ageing on PUU

Fig. 6a, b and c show different regions of the FTIR spectra from the blank PUU after UV ageing for different times, with the major changes in FTIR spectra of different PUU samples after UV ageing shown in Table 3. In the region from 3700–2200 cm^{-1} (Fig. 6a), UV irradiation led to the emergence of several new peaks at 3467 cm^{-1}, 3204 cm^{-1}, and 3055 cm^{-1}, which are considered to represent the stretching vibration of N-H bonds in primary and secondary amine and imine groups [43]. Meanwhile, the peak intensities in the region from 3000–2800 cm^{-1} greatly decreased especially after 24 h, indicating oxidation of methylene and methyl groups in both aliphatic and aromatic structures. These changes are in agreement with the broadened peak in the whole region (3700–2200 cm^{-1}) resulting from the formation of different types of N-H and O-H groups [19, 43, 44].

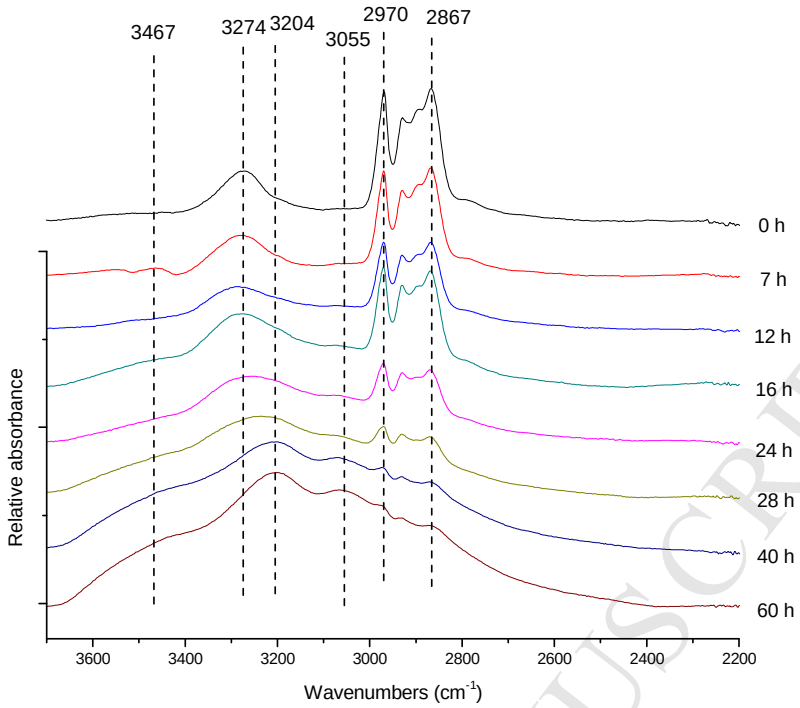

298

299 (a)

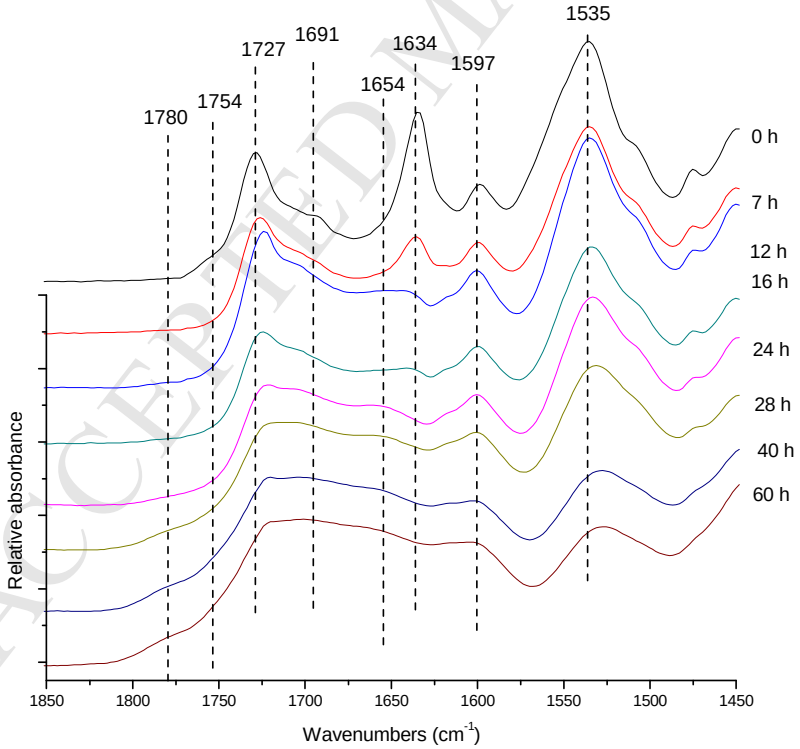

300

301 (b)

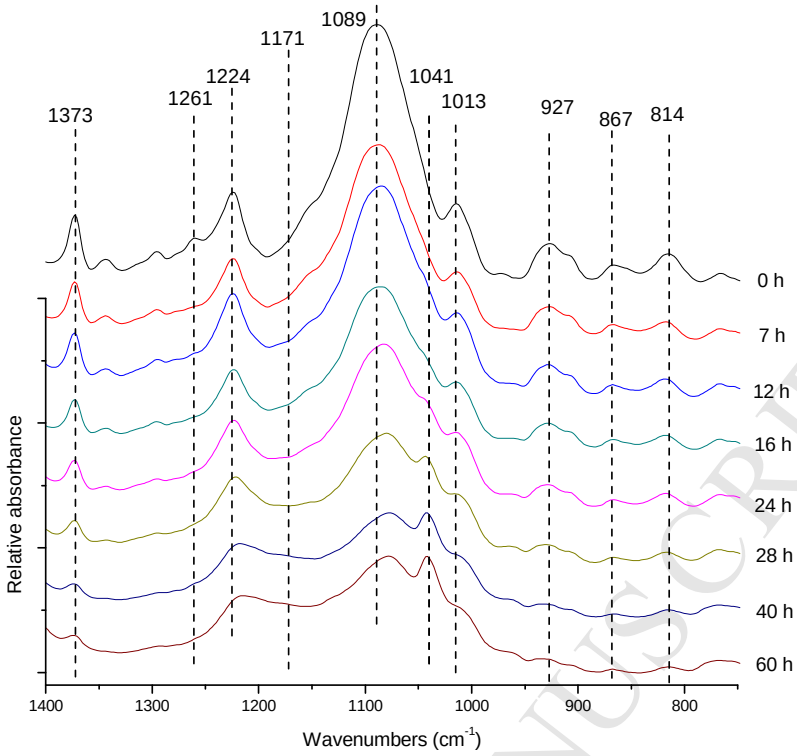

302

303 (c)

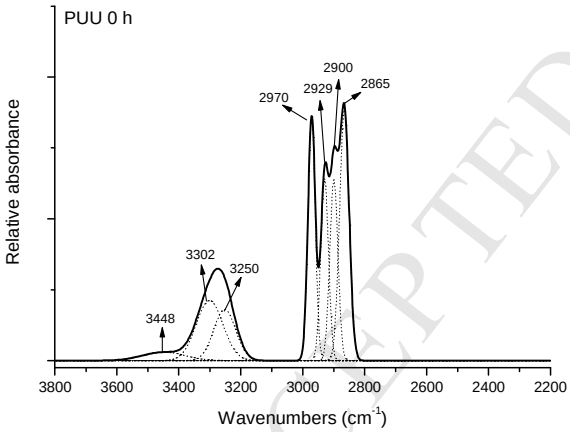

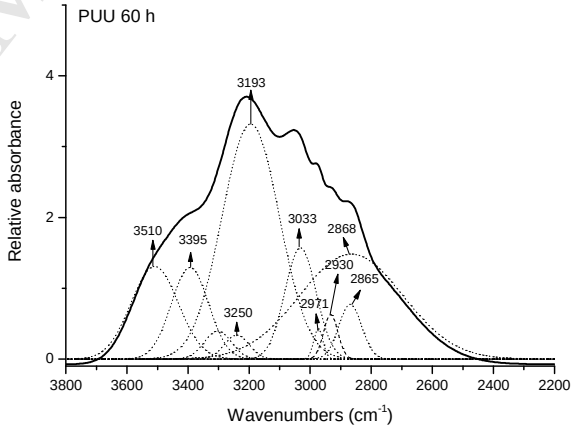

304

305 (d) (e)

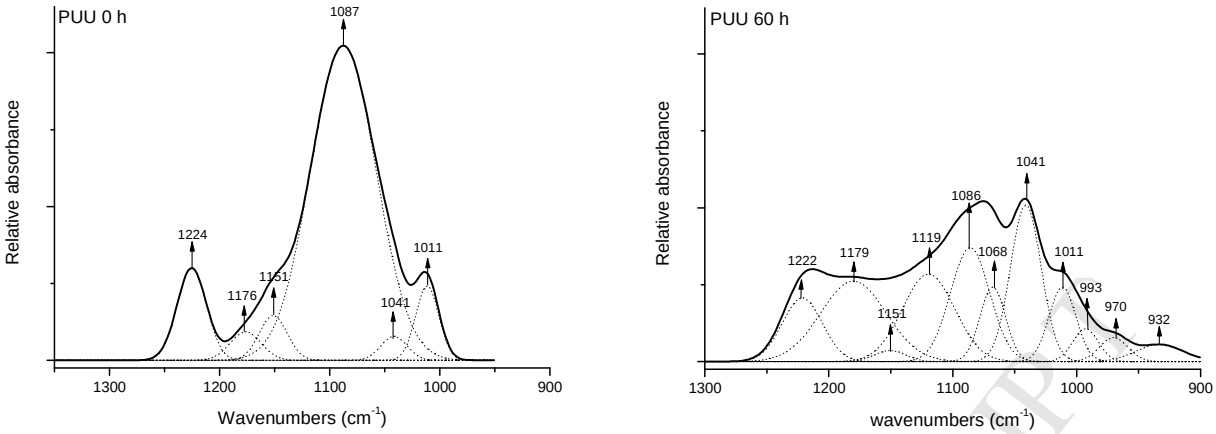

306

307 (f) (g)

308 Fig. 6. FTIR spectra of the blank PUU sample after 0 h, 7 h, 12 h, 16 h, 24 h, 28 h, 40 h and
309 60 h of UV ageing in the regions: 3700–2200 cm^{-1} (a), 1850–1450 cm^{-1} (b), and 1400–
310 750 cm^{-1} (c); Band-fitted FTIR spectra of the blank PUU samples in the region of 3800–
311 2200 cm^{-1} before (d) and after (e) 60 h of UV ageing; and band-fitted FTIR spectra from the
312 blank PUU samples in the region from 1350–900 cm^{-1} before (f) and after (g) 60 h of UV
313 ageing.

314

315 Table 3. Changes in FTIR spectra of PUU materials after 60 h of UV ageing.

Peak area (cm^{-1})	Peak centre (cm^{-1})	Change[a]	Assignment[b]
3700–2200	3510	a	υ (N-H) in free primary amines
	3390	a	υ (N-H) in free secondary amines
	3302	de	υ (N-H) in urethane group
	3250	de	υ (N-H) in urea group
	3190	a	υ (N-H) in hydrogen-bonded primary/ secondary amines
	3033	a	υ (N-H) in imines
	2970	de	υ^{as} ($-CH_3$)
	2929	de	υ^{s} ($-CH_3$)
	2902	de	υ^{as} ($-CH_2$)
	2867	de	υ^{s} ($-CH_2$)

1850–1450	1780	a	υ (C=O) in peresters/anhydrides
	1754	in	υ (C=O) free
	1727 (move to 1720)	in	υ (C=O) free and hydrogen-bonded
	1691	in	υ (C=O) hydrogen-bonded
	1690–1640	a	υ (C=N) in imines
	1654	a	δ (N-H) shoulder in primary amines
	1634	de	υ (C=O) in diphenylurea group
	1597	de	υ (C=C) in aromatic ring
	1536	d	δ (N-H) + υ (C-N) + υ (C-C) Amide II in urethane & urea groups combined
1400–750	1373	de	υ (C-N)
	1261	de	υ (C-N) in urea
	1222	de	υ (C-N) in urethane (Amide III)
	1176	a	υ^{as} (C-O) in esters
	1086	de	υ^{as} (C-O-C) in ethers
	1043	a	υ^{s} (C-O) in esters
	927	de	υ^{s} (C-O-C) in ethers
	867	de	υ (C-O-C)/ρ ($-CH_2$) from ethers
	814	de	δ_{oop} (C-H) in aromatic ring

[a] a = appear; d = disappear; in = increase of intensity; de = decrease of intensity.

[b] υ, Stretching vibration; δ, in plane deformation vibration, δ_{oop}, out of plane deformation vibration

An additional analysis of the FTIR region from 3000–2800 cm^{-1} was performed through band fitting using the Gaussian method. The band-fitted peaks before and after 60 h of UV ageing are shown in Fig. 6d and e, respectively. It can be seen that both the peaks representing the N-H bonds in the urethane (at 3302 cm^{-1}) and in the urea (at 3250 cm^{-1}) decreased in intensity after 60 h of UV ageing. The peaks at 3510 cm^{-1}, 3390 cm^{-1}, 3190 cm^{-1} and 3033 cm^{-1} are speculated to represent the N-H stretching vibration of free primary amines, free secondary amines, hydrogen-bonded primary/secondary amines, and imines.

In the region from 1850–1450 cm^{-1} (Fig. 6b), urea bonds (-NH-CO-NH-) at 1634 cm^{-1} rapidly decreased during the first 7 h, indicating a significant initial loss of urea bonds in the early stage of

UV ageing for the blank PUU. This peak had almost disappeared after 12 h. The peak at 1261 cm^{-1} (Fig. 6c), which represents the C-N stretching vibration in the urea bond, also decreased quickly, and almost disappeared within the first 7 h. The Amide II peak at 1536 cm^{-1} (Fig. 6b) decreased slightly within the first 24 h then decreased rapidly until 28 h, suggesting a substantial decomposition of the urethane bonds in the blank PUU. Meanwhile, the characteristic peaks of the benzene ring (the C=C stretching vibration at 1597 cm^{-1} and the C-H out-of-plane deformation vibration at 814 cm^{-1}) (Fig. 6c) were also reduced after exposure to UV for 28 h, indicating a loss of aromatic groups on the sample surface. As a result, the loss of the aromatic urethane structure as indicated by both the urethane and aromatic groups suggests possible chain scission and photo-Fries rearrangement of the urethane group during photodegradation [43, 45, 46]. Meanwhile, a new shoulder appearing at 1654 cm^{-1} could be recognised as the deformation of N-H bonds in primary amine groups formed during UV ageing [47]. In the carbonyl region, the main C=O stretching vibration peaks slightly increased and shifted from 1727 cm^{-1} to 1720 cm^{-1}, while the peaks at 1754 cm^{-1} and 1691 cm^{-1} increased steadily during ageing, indicating that both free and hydrogen-bonded C=O groups were formed. The increase in intensity in the spectral region between 1690 cm^{-1} and 1640 cm^{-1} is proposed to be due to the formation of imine groups (stretching vibration of C=N). In addition, a new peak at 1780 cm^{-1} appeared after 24 h of UV ageing. This new peak could be due to the C=O stretching vibration in perester or anhydride groups produced during the photooxidation, which is consistent with the XPS results. These changes are all likely to be related to the oxidation of ether groups in soft segments well as the urethane/urea groups in hard segments of the PUU elastomer [19, 48-50].

In the region from 1400–750 cm^{-1} (Fig. 6c), the relative decrease in absorbance of the C-N stretching vibration at 1373 cm^{-1} and Amide III peak at 1222 cm^{-1} are similar to that of the Amide II peak in Fig. 6b. Characteristic peaks from ether groups are due to the C-O-C asymmetrical stretching vibration, which occur at 1086 cm^{-1} for these materials. During UV ageing of the blank PUU, this

peak, along with the peaks at 927 cm^{-1} and 867 cm^{-1} representing the C-O-C symmetrical stretching vibration and the coupled C-O stretching vibration in the ether group, kept decreasing [41, 42]. As the characteristic peaks for ether groups decreased, two new peaks emerged, one being a shoulder at 1171 cm^{-1}, with the other at 1043 cm^{-1}. These two newly-formed peaks could be the double peaks of asymmetrical and symmetrical C-O peaks from aliphatic esters, which are formed as oxidation products of the ether groups in soft segments [50-52]. UV ageing also caused the consistent movement of the peak for the C-O-C asymmetrical stretching vibration from 1086 cm^{-1} to 1076 cm^{-1}, suggesting possible chain scission and crosslinking reactions between the ether chains in soft segments [37, 53, 54].

To better understand the modification of the C-O structure in soft segments of the PUU, band fitting was performed on the FTIR spectra in the region from 1350–900 cm^{-1} before and after 60 h of UV ageing, with the results shown in Fig. 6f and g, respectively. The blank PUU without UV ageing showed a peak at 1087 cm^{-1}, which is proposed to be due to the asymmetrical stretching vibration of the C-O-C bond in the polyether groups of PUU. After band fitting, there were two peaks at 1041 cm^{-1} and 1176 cm^{-1}, which likely represent the asymmetrical and symmetrical stretching vibration of C-O-C bonds in ester groups formed during UV ageing by oxidation of the ether groups. After 60 h of UV ageing, these peaks at 1041 cm^{-1} and 1176 cm^{-1} had a dramatic increase, while the peaks at 1068 cm^{-1} reduced significantly. These changes indicate that significant amounts of ester groups formed from ether groups. Meanwhile, a new peak emerged at 1068 cm^{-1}, suggesting that a new type of ether group had formed in the aged PUU sample. The new ether groups might have resulted from crosslinking generated by radicals on the C-O-C chain under UV irradiation. In addition, UV ageing led to the appearance of several new peaks between 900 cm^{-1} to 1000 cm^{-1}, namely, peaks at 993 cm^{-1}, 970 $cm^{-1,}$ and 932 cm^{-1}, indicating the formation of some -OH group-containing products, such as carboxylic acids and alcohols.

3.4.3 Effect of carbon black addition on the UV stability of PUU

Fig. 7 shows representative results for carbon black-containing samples. Fig. 7a compares the spectra of the blank PUU and PUU-C3 in the region from 1800–700 cm^{-1}. It can be seen that the peaks due to C=O and C-N stretching vibrations of urea groups at 1637 cm^{-1} and 1261 cm^{-1}disappeared in the blank PUU. However, these peaks remained to some extent in the PUU-C3 sample after 12 h of UV irradiation, indicating that carbon black provided some protection to the polymer in the early stages of UV ageing. Fig. 7b shows the spectra in the region from 3700–750 cm^{-1} comparing PUU and PUU-C3 after 40 h ageing. The peak representing urea bonds could not be seen for both the blank PUU and PUU-C3. However, PUU-C3 appeared to suffer less from UV damage than the blank PUU as shown by the large amounts of the original structure remaining (aromatic ring at 1597 cm^{-1} and 811 cm^{-1}; and aliphatic ether at 1079 cm^{-1}) and the low content of oxidation products detected (carbonyl group at 1708 cm^{-1} and amine group at 3502 cm^{-1})

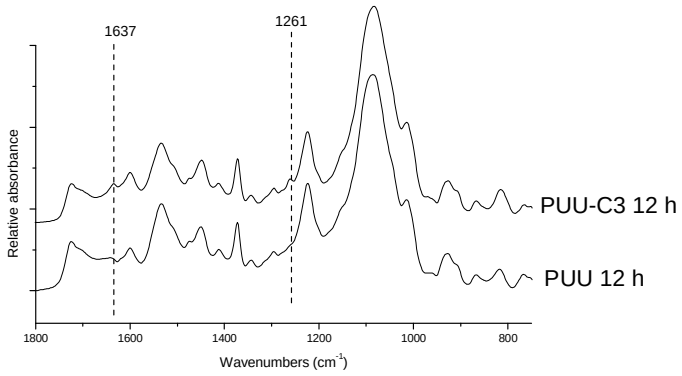

390

391 (a)

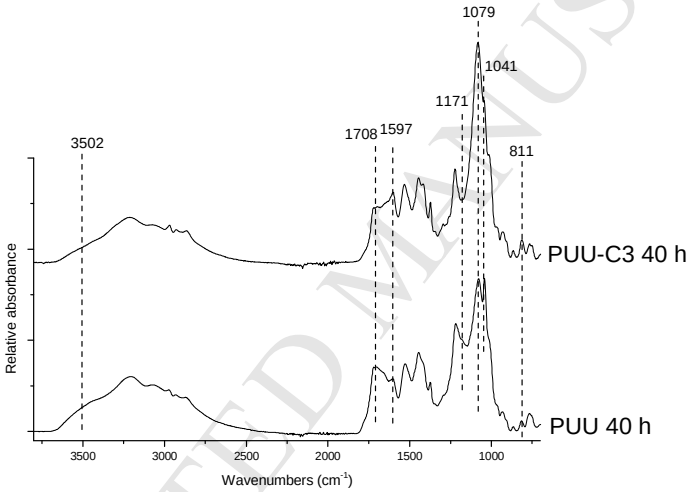

392

393 (b)

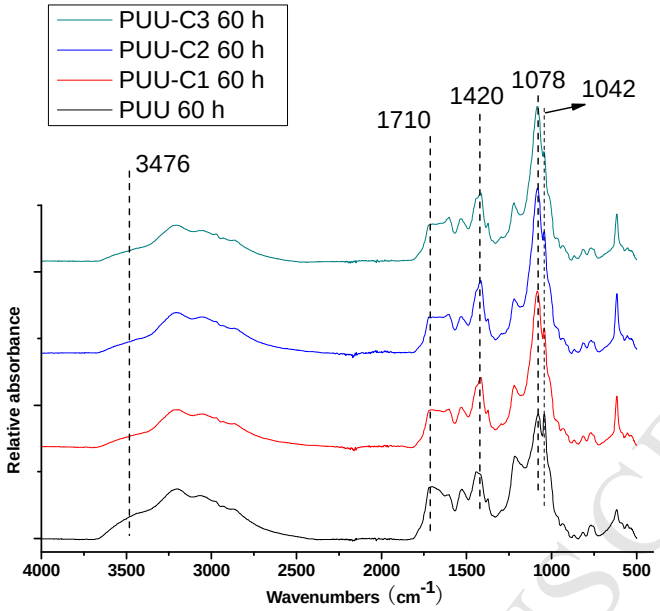

(c)

Fig. 7. FTIR spectra of (a) PUU and PUU-C3, aged for 12 h; (b) PUU and PUU-C3, aged for 40 h; and (c) PUU, PUU-C1, PUU-C2 and PUU-C3, aged for 60 h.

To compare the degree of photoinduced changes in different samples, the FTIR spectra of the blank PUU, PUU-C1, PUU-C2 and PUU-C3 aged for 60 h were collected and are shown in Fig. 7c. The aged PUU sample had increased peaks at 3476 cm^{-1} (υ (N-H)), 1710 cm^{-1} (υ (C=O)) and 1042 cm^{-1} (υ^{s} (C-O) in esters) and decreased peaks at 1420 cm^{-1} (δ ($-CH_2$)) and 1078 cm^{-1} (υ^{as} (C-O-C) in ethers). The carbon black-containing samples present less significant changes than the sample without carbon black, indicating lower degrees of oxidation in the soft segments and less degradation in the hard segments when carbon black is present. The relative degrees of photoinduced changes in the hard segments and soft segments have been assessed using two indices that were calculated using peak areas from band-fitted spectra. The hard segment irradiation index (HSII) (Fig. 8) was calculated using the ratio of the area of the UV-generated peaks for the N-H bonds of primary

409 amines (3508 cm^{-1}, 3371 cm^{-1} and 3184 cm^{-1}) to the area of the peak for the original N-H bonds in
410 the urethane/urea linkages (3302 cm^{-1} and 3250 cm^{-1}). The soft segment irradiation index (SSII)
411 (Fig. 8b) was calculated using the ratio of the area of ester peaks (1179 cm^{-1} and 1041 cm^{-1}) and
412 branched ether bond peaks (1119 cm^{-1} and 1068 cm^{-1}) formed during UV ageing, to the area of the
413 original ether peaks (1086 cm^{-1} and 1076 cm^{-1}). Changes in the hard segments and soft segments
414 after 60 h of UV ageing with carbon black as a UV stabiliser were 44% and 32% of the respective
415 values without carbon black, with the PUU sample containing carbon black C3 again showing the
416 least degradation.

417

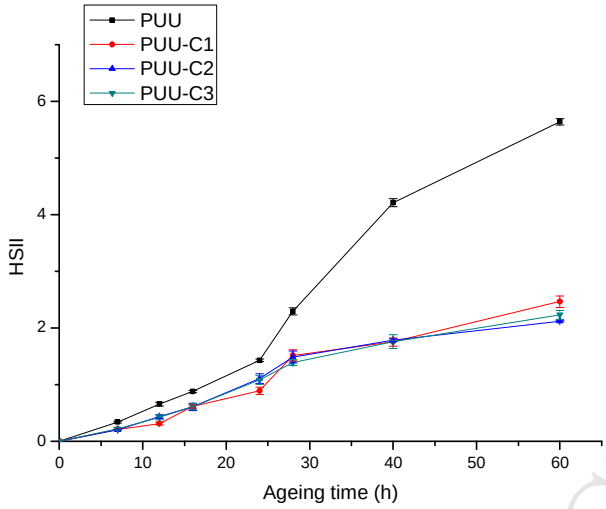

418

419 (a)

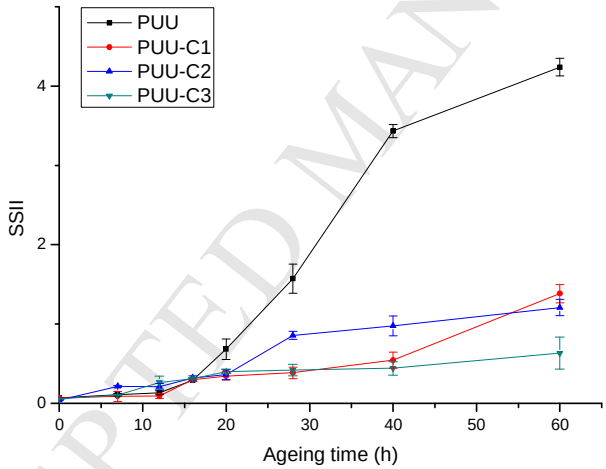

420

421 (b)

422 Fig. 8. HSII (a) and SSII (d) changes based on FTIR spectra of PUU, PUU-C1, PUU-C2

423 and PUU-C3 aged for 60 h.

424

3.5 DSC

Fig. 9 shows the DSC results for the different PUU samples before and after UV irradiation for 60 h. For all the samples, there was a glass transition (T_g) for the soft segments at −48°C and a melting transition (T_m) of the soft segments at about 9°C. A T_g at a higher temperature of about 44°C was shown, which could be ascribed to the hard segments [56]. The absence of a melting transition at higher temperature suggests that the hard segments based on TDI in this work were not flexible enough for chain alignment and the formation of crystallites. It is possible that crosslinking during cure restricted chain movement and the formation of a crystalline structure [57].

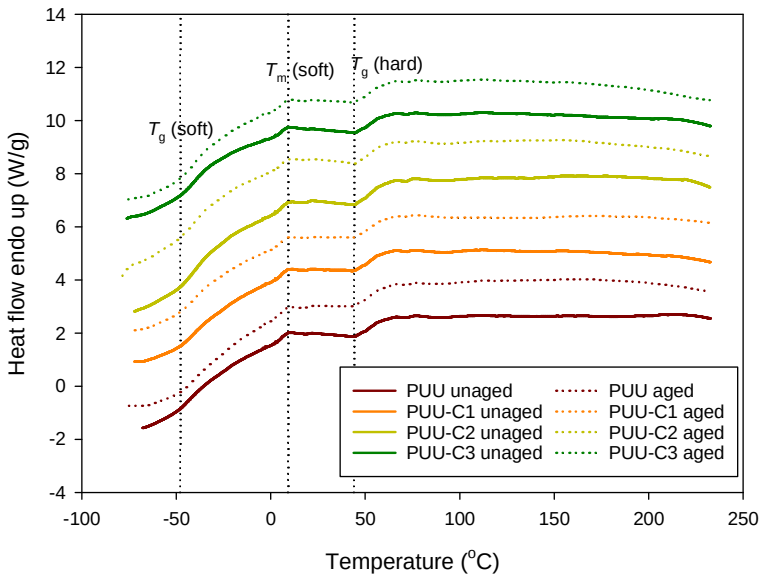

Fig. 9. DSC results for different PUU samples, unaged and aged.

The PUU samples showed almost identical DSC curves (Fig. 9), suggesting that neither the carbon black type nor UV exposure had any apparent impact on the thermal properties of the samples. Previous studies [58, 59] have reported that photoageing could reduce the ability of elastomers to crystallise due to crosslinking. Here, our results indicate that although UV irradiation did cause

variation in the surface molecular structure, these changes were not significant enough to affect the bulk thermal properties of the polymer. Higher exposure times would likely reduce the enthalpy and temperature of the crystalline melting peak or recrystallisation exothermic peak.

4 Conclusions

The photodegradation of aromatic PUUs is a complicated process that requires further study to completely elucidate the mechanism of degradation and determine the best approach to stabilisation. In this study, crosslinked segmented PUU samples were prepared with and without different types of carbon black as the UV stabiliser, and the resulting samples were then exposed to low doses of UVA at 50°C up to a total dose of 157.68 kJ/m^2 at 340 nm. SEM, XPS, FTIR and DSC analyses were applied to investigate the changes in the UV-aged samples.

From the XPS and FTIR analyses, urea groups were found to be the most UV-sensitive, showing early degradation during the ageing of the PUU, most likely due to chain scission and photo-Fries rearrangement via direct UV absorption of the aromatic groups. Aliphatic ether groups were also found to be very sensitive to UV irradiation, leading to the formation of anhydride or perester groups via photooxidation.

Carbon black provided moderate UV protection for PUU elastomers, especially in preventing oxidation of aliphatic ether groups, with results from XPS and SEM analyses suggesting that the carbon black with a smaller particle size and a higher surface area may provide better UV protection. It was shown by FTIR analyses that the degrees of photoinduced changes in the hard segments and soft segments after 60 h where carbon black was used as a UV stabiliser were 44% and 32% of the respective values without carbon black.

Results from DSC analysis suggested that changes in the samples due to UV degradation were restricted to the surface, with bulk thermal properties unaffected.

Based on the data collected here, recommendations to improve the UV weathering performance of PUUs include: reducing the urea content; using small particle size, high surface area carbon black additives; increasing carbon black content to protect against direct UV absorption of aromatic groups; and, the introduction of hindered amine stabilisers to protect against photooxidation, particularly of aliphatic ether groups.

Acknowledgments

The authors acknowledge financial support from the Defence Materials Technology Centre (DMTC), which was established and is supported by the Australian Government's Defence Future Capability Technology Centre (DFCTC) initiative. The authors would also like to acknowledge the Australian Microscopy & Microanalysis Research Facility at the Centre for Microscopy and Microanalysis (CMM), The University of Queensland, for use of facilities and scientific and technical assistance.

References

[1] C. Hepburn, Polyurethane Elastomer Chemistry, Polyurethane Elastomers, Springer Netherlands, Dordrecht, 1992, pp. 29-50.

[2] E. Sharmin, F. Zafar, Polyurethane: An Introduction, in: F. Zafar, E. Sharmin (Eds.), Polyurethane, InTech2012.

484 [3] T.K. Chen, Y.I. Tien, K.H. Wei, Synthesis and characterization of novel segmented
485 polyurethane/clay nanocomposites, Polymer 41(4) (2000) 1345-1353.

486 [4] M. Burke, D. Townend, Acoustic and mechanical properties of polyurethanes based on
487 polybutadiene soft segment, Plastics, Rubber and Composites 28(5) (1999) 185-190.

488 [5] Y. Liu, Y. Liu, S. Liu, H. Tan, Effect of accelerated xenon lamp aging on the mechanical
489 properties and structure of thermoplastic polyurethane for stratospheric airship envelope, Journal of
490 Wuhan University of Technology-Mater. Sci. Ed. 29(6) (2014) 1270-1276.

491 [6] X. Yang, C. Vang, D. Tallman, G. Bierwagen, S. Croll, S. Rohlik, Weathering degradation of a
492 polyurethane coating, Polymer Degradation and Stability 74(2) (2001) 341-351.

493 [7] J.M. Powers, M.B. Moffett, J.C. McGrath, Broadband, acoustically transparent, nonresonant
494 PVDF hydrophone, The United States Of America As Represented By The Secretary Of The Navy,
495 US, 1988.

496 [8] N. Lagakos, J.A. Bucaro, Planar and linear fiber optic acoustic sensors embedded in an elastomer
497 material, The United States Of America As Represented By The Secretary Of The Navy, US, 1994.

498 [9] H. Aglan, M. Calhoun, L. Allie, Effect of UV and hygrothermal aging on the mechanical
499 performance of polyurethane elastomers, Journal of Applied Polymer Science 108(1) (2008) 558-564.

500 [10] S. Zhang, Z. Ren, S. He, Y. Zhu, C. Zhu, FTIR spectroscopic characterization of polyurethane-
501 urea model hard segments (PUUMHS) based on three diamine chain extenders, Spectrochimica Acta
502 Part A: Molecular and Biomolecular Spectroscopy 66(1) (2007) 188-193.

503 [11] G. Oertel, L. Abele, Polyurethane Handbook: Chemistry, Raw Materials, Processing,
504 Application, Properties, Hanser1994.

505 [12] G. Stack, J. Miller, E. Chang, Development of seawater‐resistant polyurethane elastomers for
506 use as sonar encapsulants, Journal of Applied Polymer Science 42(4) (1991) 911-923.

507 [13] M. van der Schuur, B. Noordover, R.J. Gaymans, Polyurethane elastomers with amide chain
508 extenders of uniform length, Polymer 47(4) (2006) 1091-1100.

509 [14] A.K. Bhowmick, H. Stephens, Handbook of elastomers, CRC Press2000.

510 [15] X. Qin, J. Xiong, X. Yang, X. Wang, Z. Zheng, Preparation, morphology, and properties of
511 polyurethane–urea elastomers derived from sulphone-containing aromatic diamine, Journal of
512 Applied Polymer Science 104(6) (2007) 3554-3561.

513 [16] A.K. Mishra, D. Chattopadhyay, B. Sreedhar, K. Raju, Thermal and dynamic mechanical
514 characterization of polyurethane–urea–imide coatings, Journal of Applied Polymer Science 102(4)
515 (2006) 3158-3167.

516 [17] V. Thomas, M. Jayabalan, A new generation of high flex life polyurethane urea for polymer
517 heart valve—studies on in vivo biocompatibility and biodurability, Journal of Biomedical Materials
518 Research Part A 89(1) (2009) 192-205.

519 [18] H. Shirasaka, S.-i. Inoue, K. Asai, H. Okamoto, Polyurethane urea elastomer having
520 monodisperse poly (oxytetramethylene) as a soft segment with a uniform hard segment,
521 Macromolecules 33(7) (2000) 2776-2778.

522 [19] C.E. Hoyle, H. Shah, K. Moussa, Photolysis of Methylene 4,4'-Diphenyldiisocyanate-Based
523 Polyurethane Ureas and Polyureas, Polymer Durability, American Chemical Society1996, pp. 91-111.

524 [20] W.L. Hawkins, Stabilization Against Degradation by Radiation, Polymer Degradation and
525 Stabilization, Springer Berlin Heidelberg, Berlin, Heidelberg, 1984, pp. 74-90.

526 [21] J.M. Funt, W.L. Sifleet, M. Tomme, Carbon black in plastics, in: J.-B. Donnet, R.C. Bansal, M.-
527 J. Wang (Eds.), Carbon Black: Science and Technology, Second Edition, Marcel Dekker Inc, New
528 York, USA, 1993, p. 461.

529 [22] J.V. Accorsi, The Impact of Carbon Black Morphology and Dispersionon the Weatherability of
530 Polyethylene, KGK Kautschuk Gummi Kunststoffe 54(6) (2001) 321-326.

531 [23] S.W. Bigger, O. Delatycki, The effects of pigments on the photostability of polyethylene,
532 Journal of Materials Science 24(6) (1989) 1946-1952.

533 [24] M. Liu, A.R. Horrocks, Effect of Carbon Black on UV stability of LLDPE films under artificial
534 weathering conditions, Polymer Degradation and Stability 75(3) (2002) 485-499.

535 [25] V. Wallder, W. Clarke, J.B. DeCoste, J. Howard, Weathering studies on polyethylene, Industrial
536 & Engineering Chemistry 42(11) (1950) 2320-2325.

537 [26] J. Howard, H. Gilroy, Natural and artificial weathering of polyethylene plastics, Polymer
538 Engineering & Science 9(4) (1969) 286-294.

539 [27] T. Ramotowski, K. Jenne, NUWC XP-1 polyurethane-urea: a new, "acoustically transparent"
540 encapsulant for underwater transducers and hydrophones, OCEANS 2003. Proceedings, 2003, pp.
541 227-230 Vol.1.

542 [28] J.F. Rabek, Photo-Oxidative Degradation, Photodegradation of Polymers: Physical
543 Characteristics and Applications, Springer Berlin Heidelberg, Berlin, Heidelberg, 1996, pp. 51-97.

544 [29] F. Liu, Y. Hao, Z. Wang, H. Shi, E. Han, W. Ke, Flaking and degradation of polyurethane
545 coatings after 2 years of outdoor exposure in Lhasa, Chinese Science Bulletin 55(7) (2010) 650-655.

546 [30] A. Rekondo, M.J. Fernández-Berridi, L. Irusta, Photooxidation and stabilization of silanised
547 poly(ether-urethane) hybrid systems, Polymer Degradation and Stability 92(12) (2007) 2173-2180.

548 [31] R. Marchant, Q. Zhao, J. Anderson, A. Hiltner, Degradation of a poly (ether urethane urea)
549 elastomer: infra-red and XPS studies, Polymer 28(12) (1987) 2032-2039.

550 [32] O.G. Tarakanov, L.V. Nevskji, V.K. Beljakov, Photodestruction and photooxidative destruction
551 of polyurethanes, Journal of Polymer Science Part C: Polymer Symposia 23(1) (1968) 193-199.

552 [33] M. Rashvand, Z. Ranjbar, S. Rastegar, Nano zinc oxide as a UV-stabilizer for aromatic
553 polyurethane coatings, Progress in Organic Coatings 71(4) (2011) 362-368.

554 [34] Y. Deslandes, G. Pleizier, D. Alexander, P. Santerre, XPS and SIMS characterisation of
555 segmented polyether polyurethanes containing two different soft segments, Polymer 39(11) (1998)
556 2361-2366.

557 [35] S.-J. Park, K.-S. Cho, S.-K. Ryu, Filler–elastomer interactions: influence of oxygen plasma
558 treatment on surface and mechanical properties of carbon black/rubber composites, Carbon 41(7)
559 (2003) 1437-1442.

560 [36] R. Ogawa, J. Watanabe, K. Ishihara, Domain-controlled polymer alloy composed of segmented
561 polyurethane and phospholipid polymer for biomedical applications, Science and Technology of
562 Advanced Materials 4(6) (2003) 523-530.

563 [37] Y. Wu, Y.-Y. Cao, S.-P. Wu, Z.-F. Li, Preparation and properties of adjacency crosslinked
564 polyurethane-urea elastomers, Frontiers of Materials Science 6(4) (2012) 347-357.

565 [38] Z.-F. Li, Y. Wu, F.-T. Zhang, Y.-Y. Cao, S.-P. Wu, T. Wang, Preparation and properties of poly
566 HTBN-based urethane-urea/organo reactive montmorillonite nanocomposites, Frontiers of Materials
567 Science 6(4) (2012) 338-346.

568 [39] E. Ayres, W.L. Vasconcelos, R.L. Oréfice, Attachment of inorganic moieties onto aliphatic
569 polyurethanes, Materials Research 10(2) (2007) 119-125.

570 [40] S.-K. Wang, C.S.P. Sung, Spectroscopic Characterization of Model Urea, Urethane Compound,
571 and Diamine Extender for Polyurethane− Urea, Macromolecules 35(3) (2002) 877-882.

572 [41] A. Sánchez-Ferrer, D. Rogez, P. Martinoty, Synthesis and characterization of new polyurea
573 elastomers by sol/gel chemistry, Macromolecular Chemistry and Physics 211(15) (2010) 1712-1721.

574 [42] A.K. Mishra, D. Chattopadhyay, B. Sreedhar, K. Raju, FT-IR and XPS studies of polyurethane-
575 urea-imide coatings, Progress in Organic Coatings 55(3) (2006) 231-243.

576 [43] D. Rosu, L. Rosu, C.N. Cascaval, IR-change and yellowing of polyurethane as a result of UV
577 irradiation, Polymer Degradation and Stability 94(4) (2009) 591-596.

578 [44] R.P. Singh, N.S. Tomer, S.V. Bhadraiah, Photo-oxidation studies on polyurethane coating:
579 effect of additives on yellowing of polyurethane, Polymer Degradation and Stability 73(3) (2001)
580 443-446.

581 [45] L.Q. Wang, G.Z. Liang, G.C. Dang, F. Wang, X.P. Fan, W.B. Fu, Photochemical Degradation
582 Study of Polyurethanes as Relic Protection Materials by FTIR‐ATR, Chinese Journal of Chemistry
583 23(9) (2005) 1257-1263.

584 [46] B. Thapliyal, R. Chandra, Advances in photodegradation and stabilization of polyurethanes,
585 Progress in Polymer Science 15(5) (1990) 735-750.

586 [47] A. Ludwick, H. Aglan, M.O. Abdalla, M. Calhoun, Degradation behavior of an ultraviolet and
587 hygrothermally aged polyurethane elastomer: Fourier transform infrared and differential scanning
588 calorimetry studies, Journal of Applied Polymer Science 110(2) (2008) 712-718.

589 [48] C.E. Hoyle, H. Shah, K. Moussa, P. Berry, I.B. Rufus, Photodegradation of MDI Based
590 Polyurethane/Urea Elastomers, University Of Southern Mississippi Hattiesburg Dept of Polymer
591 Science, 1993.

592 [49] C. Wilhelm, J.-L. Gardette, Infrared analysis of the photochemical behaviour of segmented
593 polyurethanes: 1. Aliphatic poly (ester-urethane), Polymer 38(16) (1997) 4019-4031.

594 [50] M.A. Schubert, M.J. Wiggins, J.M. Anderson, A. Hiltner, Role of oxygen in biodegradation of
595 poly (etherurethane urea) elastomers, Journal of Biomedical Materials Research Part A 34(4) (1997)
596 519-530.

597 [51] C. Wilhelm, J.-L. Gardette, Infrared analysis of the photochemical behaviour of segmented
598 polyurethanes: aliphatic poly (ether-urethane) s, Polymer 39(24) (1998) 5973-5980.

599 [52] S.J. McCarthy, G.F. Meijs, N. Mitchell, P.A. Gunatillake, G. Heath, A. Brandwood, K.
600 Schindhelm, In-vivo degradation of polyurethanes: transmission-FTIR microscopic characterization
601 of polyurethanes sectioned by cryomicrotomy, Biomaterials 18(21) (1997) 1387-1409.

602 [53] E.M. Christenson, J.M. Anderson, A. Hiltner, Oxidative mechanisms of poly (carbonate
603 urethane) and poly (ether urethane) biodegradation: in vivo and in vitro correlations, Journal of
604 Biomedical Materials Research Part A 70(2) (2004) 245-255.

605 [54] M. Rus, Z. Anika, T.J. Kemp, A.J. Clark, Degradation studies of polyurethanes based on
606 vegetable oils. Part 1. Photodegradation, Progress in Reaction Kinetics and Mechanism 33(4) (2008)
607 363-391.

608 [55] H.-F. Lee, H.H. Yu, Study of electroactive shape memory polyurethane-carbon nanotube
609 hybrids, Soft Matter 7(8) (2011) 3801-3807.

610 [56] C.E. Hoyle, C.P. Chawla, K.-J. Kim, The effect of flexibility on the photodegradation of
611 aromatic diisocyanate-based polyurethanes, Journal of Polymer Science Part A: Polymer Chemistry
612 26(5) (1988) 1295-1306.

613 [57] J.-F. Pilichowski, T. Liptaj, M. Morel, E. Terriac, M. Baba, Cross-linking of polybutadiene:
614 correlation between solid-state 1H NMR spectroscopy, thermoporosimetry, densimetry and
615 crystallinity measurements, Polymer International 52(12) (2003) 1913-1918.

616 [58] M. Baba, S. George, J.L. Gardette, J. Lacoste, Crosslinking of elastomers upon ageing: a kinetic
617 approach based on crystallinity changes followed by DSC, Polymer International 52(6) (2003) 863-
618 868.

619 [59] M. Morel, J. Lacoste, M. Baba, Photo-DSC I: A new tool to study the semi-crystalline polymer
620 accelerated photo-ageing, Polymer 46(22) (2005) 9274-9282.

621 [60] Z.S. Petrović, Z. Zavargo, J.H. Flyn, W.J. Macknight, Thermal degradation of segmented
622 polyurethanes, Journal of Applied Polymer Science 51(6) (1994) 1087-1095.

623 [61] G. Trovati, E.A. Sanches, S.C. Neto, Y.P. Mascarenhas, G.O. Chierice, Characterization of
624 polyurethane resins by FTIR, TGA, and XRD, Journal of Applied Polymer Science 115(1) (2010)
625 263-268.

626 [62] D.K. Chattopadhyay, D.C. Webster, Thermal stability and flame retardancy of polyurethanes,
627 Progress in Polymer Science 34(10) (2009) 1068-1133.

628 [63] M.P. Luda, M. Guaita, O. Chiantore, Thermal degradation of polybutadiene, 2. Overall thermal
629 behaviour of polymers with different microstructures, Die Makromolekulare Chemie 193(1) (1992)
630 113-121.

631 [64] F. Chen, J. Qian, Studies on the thermal degradation of polybutadiene, Fuel Processing
632 Technology 67(1) (2000) 53-60.

633 [65] S. Benli, Ü. Yilmazer, F. Pekel, S. Özkar, Effect of fillers on thermal and mechanical properties
634 of polyurethane elastomer, Journal of Applied Polymer Science 68(7) (1998) 1057-1065.

635 [66] M. Berta, C. Lindsay, G. Pans, G. Camino, Effect of chemical structure on combustion and
636 thermal behaviour of polyurethane elastomer layered silicate nanocomposites, Polymer Degradation
637 and Stability 91(5) (2006) 1179-1191.

638

Highlights:

- ✓ Initial (60 h) photodegradation pathways of poly(urethane-urea) (PUU) was studied
- ✓ Urea groups were the most UV-sensitive, followed by aliphatic ether groups
- ✓ Carbon black provided moderate UV protection especially for aliphatic ether groups
- ✓ The smallest-sized carbon black protected PUU against degradation more effectively
- ✓ UV degradation-induced changes predominantly occurred at the surface